

Effects of a space modulation on the behavior of a 1D alternating Heisenberg spin-1/2 model

Saeed Mahdavifar¹ and Jahanfar Abouie^{2,3‡}

¹Department of Physics, University of Guilan, 41335-1914, Rasht, Iran

² Department of Physics, Shahrood University of Technology, Shahrood 36199-95161, Iran

³ School of physics, Institute for Research in Fundamental Sciences (IPM), Tehran 19395-5531, Iran

E-mail: Mahdavifar@guilan.ac.ir

E-mail: jahan@shahroodut.ac.ir

Abstract.

The effects of a magnetic field (h) and a space modulation (δ) on the magnetic properties of a one dimensional antiferromagnetic-ferromagnetic Heisenberg spin-1/2 model have been studied by means of numerical exact diagonalization of finite size systems, nonlinear sigma model and bosonization approach. The space modulation is considered on the antiferromagnetic couplings. At $\delta = 0$, the model is mapped to a gapless Luttinger liquid phase by increasing the magnetic field. However, the space modulation induces a new gap in the spectrum of the system and the system experiences different quantum phases which are separated by four critical fields. By opening the new gap a magnetization plateau appears at $\frac{1}{2}M_{sat}$. The effects of the space modulation are reflected in the emergence of a plateau in other physical functions such as the F-dimer and the bond dimer order parameters, and the pair-wise entanglement.

PACS numbers: 75.10.Jm, 75.10.Pq

‡ The authors have the same contributions in the work.

1. Introduction

The effects of a magnetic field on the magnetic properties of low-dimensional quantum magnets at zero temperature has attracted much attentions in recent years. One of the very interesting phenomena is the appearance of a magnetization plateau in the magnetization curve. This behavior can be viewed as an essentially macroscopic quantum phenomena, and has gained much attentions, recently. When a plateau is appeared the energy gap is opened, which can be in some senses regarded as a kind of generation of the Haldane conjecture [1]. In a seminal work, M. Oshikawa, M. Yamanaka and I. Affleck studied the magnetization of a general class of the Heisenberg spin chains at the presence of a magnetic field. They showed that the plateaus can be appeared when the magnetization per site m is topologically quantized by $n(s - m) = integer$, where s is the magnitude of the spin, and n is the period of the ground state determined by the explicit spatial structure of Hamiltonian [2].

The bond alternating Heisenberg spin-1/2 chains which are obtained by a space modulation in the exchange couplings [3, 4, 5, 6, 7, 8, 9] are a particular class of the low-dimensional quantum magnets to observe the magnetization plateau at zero temperature. The bond alternating Antiferromagnetic-Ferromagnetic spin-1/2 chains have a gap in the spin excitation spectrum and reveal extremely rich quantum behaviors in the presence of an external magnetic field [10, 11, 12, 13]. By turning the magnetic field, the excitation gap is reduced and reach to zero at the first critical field. Simultaneously, the magnetization start to increase up to its saturation value, 0.5 at the second critical field. More enhancement of the field re-opens the gap and the saturation plateau appears in the magnetization curve. These models have only two plateaus at zero and saturation values of the magnetization. It has been found that a space modulation in the exchange couplings can affect on the behaviors of the field induced magnetization. For example the bond alternating Ferromagnetic-Ferromagnetic-Antiferromagnetic (F-F-AF) trimerized Heisenberg spin-1/2 chains have exotic behaviors by changing the magnetic field [14]. This model can be realized in the *Cu*-compounds such as $3CuCl_2 \cdot 2dx$. The magnetization has a plateau at $\frac{M}{M_{sat}} = \frac{1}{3}$, where M and M_{sat} are the magnetization and its saturated values, respectively [15, 16]. The mid-plateaus have also been appeared in the bond alternating Ferromagnetic-Antiferromagnetic-Antiferromagnetic (F-AF-AF) trimerized Heisenberg spin-1/2 chains [17]. It has been also shown that the static structure factor dose not vary with the external magnetic field at the plateau state [18].

The other examples are the tetrameric bond-alternating Ferromagnetic-Ferromagnetic-Antiferromagnetic-Antiferromagnetic (F-F-AF-AF) Heisenberg spin models. A realization for the spin-1/2 chain with F-F-AF-AF alternations is the compound $Cu(3-Clpy)_2(N_3)_2(3-Clpy = 3-Chloroyridine)$ [19]. In such a spin- $\frac{1}{2}$ system, there is a gap from the singlet ground state to the triplet excited states in the absence of a magnetic field. At $\frac{M}{M_{sat}} = \frac{1}{2}$, a plateau is appeared in the magnetization curve by applying a magnetic field [20]. The temperature dependence of the magnetization,

magnetic susceptibility and specific heat have been also studied in the mid-plateau state of this model by means of transfer-matrix renormalization group method [21].

In this paper, by considering a different bond alternating Heisneberg spin-1/2 chain, we study the other physical properties of the mid-plateau state such as the string order and pair-wise entanglement, F-dimer and bond-dimer order parameters. The Hamiltonian of the model is

$$\begin{aligned}
 H = & -J_F \sum_{j=1}^{N/2} \mathbf{S}_{2j} \cdot \mathbf{S}_{2j+1} \\
 & + J_{AF} \sum_{j=1}^{N/2} [1 + (-1)^j \delta] \mathbf{S}_{2j-1} \cdot \mathbf{S}_{2j} - h \sum_{j=1}^N S_j^z,
 \end{aligned} \tag{1}$$

where \mathbf{S}_j is the spin- $\frac{1}{2}$ operator on the j -th site. J_F and $J_{AF}^\pm = J_{AF}(1 \pm \delta)$ denote the ferromagnetic ($J_F > 0$) and antiferromagnetic ($J_{AF} > 0$) couplings, respectively. δ is the space modulation parameter and h is proportional to the external magnetic field. The unit cell of the model has been shown in Fig. (1). The bond alternating spin-1/2

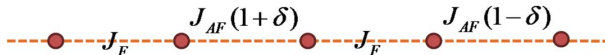


Figure 1. (Color online.) Schematic representation of a tetrameric spin chain

AF-F chains are good candidates for studying the Luttinger liquid phase. A suitable realization of the bond alternating AF-F spin chain is the Cu based $(\text{CH}_3)_2\text{NH}_2\text{CuCl}_3$ compound. Linked-cluster calculations and bulk measurements show that DMACuCl_3 is also a realization of the spin-1/2 alternating AF-F chain with nearly the same strength of antiferromagnetic and ferromagnetic couplings [22]. A space modulation changes the AF couplings alternatively and influences on the quantum properties of the system.

Using the exact diagonalization of a finite size system and employing the conformal field theory it has been already found that for $\delta \neq 0$ a magnetization plateau exist at half of the saturation value [23]. Moreover, the width of the mid-plateau is dependent to the values of δ and the critical exponent for the plateau width is obtained by the level spectroscopy method. In the present work the different properties of the model such as F-dimer and bond-dimer order parameters, string order parameter, and the pair wise entanglement of the plateau state are studied.

The outline of the paper is as follows. In the forthcoming section we discuss the model in the strong AF coupling limit and derive an effective spin chain Hamiltonian. In section III we summarize the results of the analytical field theory studies. In section IV, the results of exact diagonalization Lanczos method are presented. Finally, we discuss and summarize our results in section V.

2. Effective Hamiltonian

The easiest way to obtain the effective model, which manifestly displays mechanism for generation of the sequence of new scales is to start from the limit of noninteracting block of pairs $J_F = 0$ and strong magnetic field $h \simeq J_{AF}$ [24]. In the limiting case of the strong AF coupling $J_{AF} \gg J_F$ and $J_{AF} \gg \delta J_{AF}$ the model can be mapped to an effective spin chain Hamiltonian [12]. At $J_{AF} \gg J_F$, the system behaves as a nearly independent block of pairs. Indeed an individual block of spin pairs may be in a singlet or a triplet state with the corresponding eigenvalues given by

$$\begin{aligned} E^\pm(S) &= -\frac{3}{4}J_{AF}^\pm, \\ E^\pm(T_1) &= \frac{1}{4}J_{AF}^\pm - h, \quad E^\pm(T_0) = \frac{1}{4}J_{AF}^\pm, \\ E^\pm(T_{-1}) &= \frac{1}{4}J_{AF}^\pm + h. \end{aligned} \quad (2)$$

When h is small, the ground state consists of a product of pair singlets. As the magnetic field h increases the energy of the triplet state $|T_1\rangle$ decreases and at $h = J_{AF}^\pm$ forms together with the singlet state, a doublet of almost degenerate low energy states, split from the remaining high energy two triplet states. Thus, for a strong enough magnetic field we have a situation when the singlet $|S\rangle$ and triplet $|T_1\rangle$ states create a new effective spin $\tau = 1/2$ systems. On the new singlet-triplet subspace and up to a constant, we easily obtain the effective Hamiltonian

$$\begin{aligned} H^{eff} &= -\frac{J_F}{2} \sum_{j=1}^{N/2} [\tau_j^x \tau_{j+1}^x + \tau_j^y \tau_{j+1}^y + \frac{1}{2} \tau_j^z \tau_{j+1}^z] \\ &\quad - h_0^{eff} \sum_{j=1}^{N/2} \tau_j^z - h_1^{eff} \sum_{j=1}^{N/2} (-1)^j \tau_j^z, \end{aligned} \quad (3)$$

where $h_0^{eff} = h - J_{AF} + \frac{J_F}{4}$ and $h_1^{eff} = \delta J_{AF}$. Thus, the effective Hamiltonian is nothing but the XXZ Heisenberg chain, with anisotropy $\Delta = 1/2$ in a uniform and staggered longitudinal magnetic field. The full phase diagram of this model has been investigated by F. C. Alcaraz and A. L. Malvezzi [25] and the nature of the ground state phase transition has been pointed in Ref. [26]. The other properties also could be found in recent works such as Refs. [2, 27, 28, 29]. To find clearer picture for the low energy spectrum of the effective model (3), using the numerical Lanczos method we have computed the energy gap of the effective model. The numerical results, have been shown in Fig.2 for a chain of lengths $N = 16, 20$ and the exchange parameters $J_F = 1.0$, $J_{AF} = 9/2$, and $\delta = 1/9$. As it is seen from Fig.2, at $h_0^{eff} = 0$ or $h = J_{AF} - \frac{J_F}{4}$, the effective model reduces to the XXZ spin chain in a staggered longitudinal magnetic field. The ground state of this model is in the gapped Néel phase. By changing h_0^{eff} from zero i.e decreasing (increasing) h from the value $h = J_{AF} - \frac{J_F}{4}$, the energy gap decreases and reaches to zero at finite values of the magnetic field $h_0^{eff,-}$ ($h_0^{eff,+}$). Consequently, there is a plateau in the magnetization curve of the effective model at $0 < h_0^{eff} < h_0^{eff,+}$.

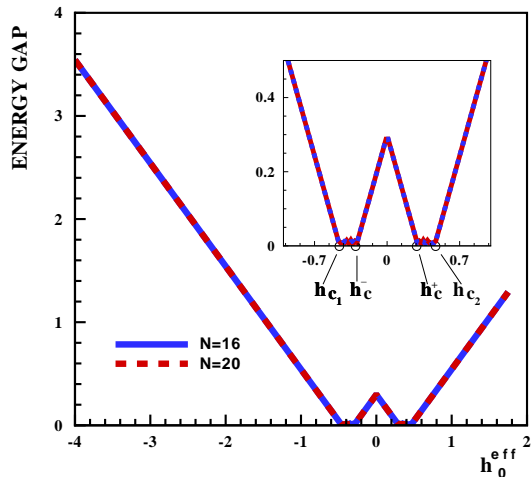


Figure 2. (Color online.) Difference between the two lowest energy levels of the effective Hamiltonian versus the magnetic field h_0^{eff} , for chains with different lengths $N = 16, 20$ and exchange parameters $J_F = 1.0$, $J_{AF} = 9/2$ and $\delta = 1/9$.

By more decreasing (increasing) of h , the energy gap remains zero down(up) to critical field $h_0^{eff,1}$ ($h_0^{eff,2}$) and, after these gapless regions it is re-opened and behaves linearly with the magnetic field h_0^{eff} . Correspondingly, in these regions the magnetization of the effective model starts to change from zero and is saturated at the critical field ($h_0^{eff,2}$).

3. Field theory predictions

In this section we will study the model (1) in the language of two continuum field theories. We have employed the nonlinear σ model and Bosonization approaches to obtain the energy gap, the critical fields and magnetization plateaus of the model.

3.1. Nonlinear σ model

The $O(3)$ nonlinear σ model (NL σ M) is a semiclassical approach which is based on the certain properties of a field theory in (1+1) dimension. In 1983 Haldane predicted theoretically the existence of a finite gap between the ground state and the first excited state of antiferromagnetic Heisenberg integer spin chains [1]. He also conjectured that the half-odd integer spin chains are gapless. The Hamiltonian of a homogeneous spin chain is mapped to a $O(3)$ NL σ M with an additional topological term. The topological term is 0 if spins of the chain are integer and π if they are half-odd integer.

Following we will investigate the low temperature behaviors of the alternating spin chain (1). For convenient on the incoming calculations let us write the Hamiltonian (1) as the following form

$$H = -J_F \sum_{j=1}^{N/4} (\mathbf{S}_{2j-1}^{(1)} \cdot \mathbf{S}_{2j-1}^{(2)} + \mathbf{S}_{2j}^{(1)} \cdot \mathbf{S}_{2j}^{(2)})$$

$$\begin{aligned}
& + J_{AF} \sum_j^{N/4} [(1 + \delta) \mathbf{S}_{2j-1}^{(2)} \cdot \mathbf{S}_{2j}^{(1)} + (1 - \delta) \mathbf{S}_{2j}^{(2)} \cdot \mathbf{S}_{2j+1}^{(1)}] \\
& + h \sum_j \mathbf{S}_j^z
\end{aligned} \tag{4}$$

where $0 \leq \delta \leq 1$. Using the spin coherent states representation for the spin operators, i.e $\mathbf{S} = s\boldsymbol{\Omega}$ we can write the Hamiltonian in terms of the classical spin vectors. By introducing three classical fields \mathbf{n} , \mathbf{L} , and $\boldsymbol{\Delta}$ the classical vectors are written as the following forms:

$$\begin{aligned}
\boldsymbol{\Omega}_{2j-1}^{(i)} &= -\mathbf{n}_{2j-1} (1 - |\frac{a}{s} \mathbf{L}_{2j-1}|^2)^{1/2} + \frac{a}{s} \mathbf{L}_{2j-1} \\
&\quad - (-1)^i \frac{a}{s} \boldsymbol{\Delta}_{2j-1}, \\
\boldsymbol{\Omega}_{2j}^{(i)} &= \mathbf{n}_{2j} (1 - |\frac{a}{s} \mathbf{L}_{2j}|^2)^{1/2} + \frac{a}{s} \mathbf{L}_{2j} + (-1)^i \frac{a}{s} \boldsymbol{\Delta}_{2j},
\end{aligned} \tag{5}$$

where $i = 1, 2$ and a is the lattice constant. Typically, for a quantum antiferromagnetic Heisenberg chain it is convenient to write the spin vectors in terms of a unimodular Néel field (\mathbf{n}) and one ferromagnetic canting field (\mathbf{L}). However for an alternating AF-F Heisenberg spin chain, the main difficulty arises from the fact that it is inhomogeneous and writing a continuous action out of the discrete Hamiltonian is not a trivial task [30]. Using another field which describes the variation of the Néel fields inside the two spin-blocks such as $\boldsymbol{\Delta}$ we can map the Hamiltonian (4) to the following $O(3)$ NL σ M:

$$\mathcal{A} = \frac{1}{2g} \int_0^L \int_0^{L_T} dx dx_0 [(\partial_x \mathbf{n})^2 + (\partial_{x_0} \mathbf{n})^2] - i\Theta W, \tag{6}$$

where W is the winding number, $L_T = c\beta$, $x_0 = c\tau$, and we have considered the case $h = 0$. By defining $\alpha = \frac{J_F}{J_{AF}}$, the coupling constant g , and the velocity of spin excitations c are given in terms of α and δ as:

$$\begin{aligned}
g &= \frac{1 - \frac{\delta^2}{2(1+\alpha)}}{s \left(1 - \frac{\delta^2}{4} - \frac{1}{2(1+\alpha)}\right)^{1/2}}, \\
c &= J_{AF} a s \left(1 - \frac{\delta^2}{4} - \frac{1}{2(1+\alpha)}\right)^{1/2}.
\end{aligned} \tag{7}$$

The topological Θ term is obtained as follow:

$$\Theta = 2\pi \left(\frac{s\delta\alpha}{1 + \alpha - \frac{\delta^2}{2}} \right), \tag{8}$$

where . For $\alpha = 0$ or $\delta = 0$ the topological Θ term is zero and the model is always gapped and the spin excitations velocity is $\frac{\sqrt{2}}{2} J_{AF} a s$. Moreover, the $\alpha = 1$ and $\delta = 0$ is the special case of AF-F Heisenberg spin chains which the topological term is always 0. This result is in good agreement with the result presented in Ref. [30]. For any other values of α and δ , the Hamiltonian is mapped to a non-integrable $O(3)$ NL σ M with Θ

in the interval $[0, \pi]$. This model is also gapped and the gap value is dependent on α and δ .

Now, let us study the model in presence of the magnetic field. Since, the model is always gapped in the absence of a magnetic field we are allowed to consider $\Theta = 0$. The Hamiltonian (4) is mapped to the following NL σ M which the effect of the magnetic field is clearly seen:

$$\mathcal{A} = \frac{1}{2g} \int d^2x [(\partial_x \mathbf{n})^2 + (\partial_{x_0} \mathbf{n} - \frac{i}{c} \mathbf{h} \times \mathbf{n})^2], \quad (9)$$

To get more physical insight from the effects of the magnetic field, it may be more physically transparent to work with two fields (θ, ϕ) where $\mathbf{n} = (\sin \theta \sin \phi, \sin \theta \cos \phi, \cos \theta)$. Here θ is co-latitude and ϕ is azimuthal angles. Selecting magnetic field in z direction, the action (9) takes the following form;

$$\mathcal{A} = \frac{1}{2g} \int d^2x \{(\partial_\mu \theta)^2 + \sin^2 \theta \left[(\phi')^2 + \frac{1}{c^2} (\phi - ih)^2 \right]\}, \quad (10)$$

where θ is the angle of \mathbf{h} and \mathbf{n} . In the term, $\mathbf{h} \times \mathbf{n}$, the magnetic field induces a hard-axis anisotropy. In other word, the magnetic field try to align all spins with \mathbf{n} in the plane normal to h . Thus for high field regime, $h > |\phi|$, the deviation of Néel field \mathbf{n} from the plane is small. Thus an expansion to quadratic order in ϑ is valid. The action is

$$\begin{aligned} \mathcal{A} = & \frac{1}{2g} \int_0^L \int_0^{L_T} d^2\mu \left(-\bar{h}^2 - \phi \partial_\mu^2 \phi - 2i\bar{h} \partial_{x_0} \phi \right. \\ & \left. + (\partial_\mu \vartheta)^2 - \vartheta^2 [(\partial_{x_0} \phi)^2 - \bar{h}^2 - 2i\bar{h} \partial_{x_0} \phi] \right), \end{aligned} \quad (11)$$

where $\bar{h} = h/c$ and the fluctuations have been separated to the in-plane and out-of-plane fluctuations.

Using a spin stiffness analysis, $1/N$ expansion and a renormalization group approach, it has been already computed the magnetization and spin correlation functions of a spin ladder in an applied magnetic field[31, 32]. The magnetization $(\sum_i \frac{\langle S_i \rangle}{N})$ is given by $M = \frac{1}{N} \frac{\partial F}{\partial h}$, where $F = -\frac{1}{\beta} \ln Z$ is the Helmholtz free energy and $Z = \int \mathcal{D}\vartheta \mathcal{D}\phi e^{-\mathcal{A}}$. The separable nature of fluctuations allows us to give the results of $M = M_o + M_i$ which is a summation of both out of plane and in plane contributions. At low enough temperatures and small value of c/h one can find that the out of plane contribution is a constant, $M_o = 1/2$, which is correspond to a uniform state. The in plane contribution has two terms, one is linear in the field and the other has a sawtooth form (See Ref. [32]). Totally, M_i is a step-like form which the width of the steps scales as $1/N$. Thus the sawtooth form is the finite size corrections and, in the thermodynamic limit $N \rightarrow \infty$ the in plane magnetization is only linear.

For our tetramerized spin chain the magnetization is given by

$$M \simeq -1 + \frac{h}{gc}. \quad (12)$$

Application of an enough high magnetic field will cause the spin alignment, or saturation with a maximum magnetization, $M_s = s$. This effect should be considered in the NL σ M

approach by a lagrange multiplier. At zero magnetic field the system is gapped and the magnetization is zero. Tuning magnetic field decreases the gap till first critical field, h_{c_1} where magnetization start to increase. At the second critical field, where the magnetization saturated, the gap reopens and spins are fully aligned in the magnetic field direction.

The critical fields which are attained by means of NL σ M are as follows:

$$\begin{aligned} h_{c_1} &= gc, \\ h_{c_2} &= \frac{3}{2}gc. \end{aligned} \tag{13}$$

3.2. Bosonization

In this section we concentrate our attentions to the low-energy and long wavelength excitations by using bosonization language. Let us consider the Hamiltonian (3). In our analysis of the model (3) we closely follow the route developed in the Ref. [27]. In the absence of both magnetic fields, $h_0^{eff} = 0$ and $h_1^{eff} = 0$ we have the XXZ spin-1/2 chain with ferromagnetic coupling and anisotropy parameter $\Delta = 1/2$. This model is critical and the long-wavelength excitations are described by the following Gaussian theory;

$$\mathcal{H} = \frac{v}{2} \int dx [(\partial_x \theta)^2 + (\partial_x \phi)^2], \tag{14}$$

where $\theta(x)$ and $\phi(x)$ are dual bosonic fields, $\partial_t \phi = v \partial_x \theta$, and satisfying the following commutation relations

$$[\phi(x), \theta(y)] = i\Theta(y - x), \tag{15}$$

$$[\phi(x), \theta(x)] = \frac{i}{2}. \tag{16}$$

v is the spin excitation's velocity and fixed by the Bethe ansatz solution as

$$v = \left(\frac{J_F}{2}\right) \frac{K}{2K-1} \sin\left(\frac{\pi}{2K}\right), \tag{17}$$

where Luttinger *parameter* K (inverse of Bosons radius [33]) is given as a function of Δ as

$$K = \frac{\pi}{2 \arccos \Delta}. \tag{18}$$

Thus K is increased monotonically along the XXZ critical line $-1 < \Delta \leq 1$ from its minimal value $K = 1/2$ (for the isotropic antiferromagnetic $\Delta = -1$ case) to unity at $\Delta = 0$ (for the noninteracting case) and goes to infinity at $\Delta = 1$ which is the ferromagnetic instability point. Meanwhile the boson radius has its maximum value $(2\pi)^{-1/2}$ for the isotropic antiferromagnetic chains and decreases by changing in Δ and goes to zero at the ferromagnetic instability point.

The maximum value of the spin excitation velocity occurs where $K \sim 1/2$ or $\Delta = -1$. It decreases monotonically by increasing K and reaches to the zero value at $K = \infty$ ($\Delta = 1$).

The continuum limit of the Hamiltonian (3) is obtained by writing spin operators in terms of bosonic fields:

$$\begin{aligned}\tau_n^z &= \sqrt{\frac{K}{\pi}} \partial_x \phi + \frac{(-1)^n a}{\pi} \sin[\sqrt{4\pi K} \phi(x)], \\ \tau_n^+ &= \frac{1}{\sqrt{2\pi}} e^{-i\sqrt{\frac{\pi}{K}} \theta(x)} ((-1)^n b \sin[\sqrt{4\pi K} \phi(x)] + c),\end{aligned}\tag{19}$$

where a , b and c are non-universal real constant in the order of unity and depends on the parameter Δ [34]. In above transformations we have made the rotation $\tau_n^\pm \rightarrow (-1)^n \tau_n^\pm$ and $\tau_n^z \rightarrow \tau_n^z$ on the standard bosonic version of the spin operators which is found extensively in the literature. Using (19), the effective Hamiltonian density is given as:

$$\begin{aligned}\mathcal{H} &= \frac{v}{2} [(\partial_x \theta)^2 + (\partial_x \phi)^2] \\ &\quad + \frac{h_1^{eff}}{\pi a_0} \sin[\sqrt{4\pi K} \phi] - h_0^{eff} \sqrt{\frac{K}{\pi}} \partial_x \phi.\end{aligned}\tag{20}$$

The mapped model is nothing but the massive sin-Gordon model with an additional topological term. Let us first consider the sin-Gordon model without the topological term $h_0^{eff} = 0$ or at the magnetic field value $h = J_{AF} - \frac{J_F}{4}$. As it has been discussed in many places, in the interval $1 < K < 2$ the spectrum of the SG model contains soliton and anti-soliton with mass \mathcal{M} . The exact relation between the soliton mass and the bare mass h_1^{eff} is as follows [35]

$$\begin{aligned}\mathcal{M} &= \mathcal{C}(K) h_1^{eff \frac{1}{2-K}}, \\ \mathcal{C}(K) &= \frac{2 \Gamma(\frac{1}{2\nu})}{\sqrt{\pi} \Gamma(\frac{1}{2} + \frac{1}{2\nu})} \left[\frac{\Gamma(1 - \frac{K}{2})}{2 \Gamma(\frac{K}{2})} \right]^{\frac{1}{2-K}}.\end{aligned}\tag{21}$$

By substituting $K = 3/2$ and $h_1^{eff} = \delta J_{AF}$ in (21) the soliton mass or equivalently the excitation gap is given as $\mathcal{M} \sim \frac{2}{J_F} (\delta J_{AF})^2$. Turning h_0^{eff} add a gradient term to the gapped SG model. This term creates a shift on the field ϕ . Actually, in the absence of the topological term the excitation spectrum of the model is gapped and the field ϕ is stucken on one of the minima where $\langle \sin \sqrt{6\pi} \rangle = -1$. This one is correspond to a staggered AF order in the effective spin chain. Tuning the uniform field h_0^{eff} the number of particle is decreased and the minima is shifted. Challenging between two uniform and staggered field causes the system experiences a different phase when $|h_0^{eff}| > \mathcal{M}$ [36]. This phase transition is occurred at h_c^- where the excitation gap reopened.

Consequently the width of the magnetization plateau is obtained as

$$h_c^+ - h_c^- \simeq \frac{4}{J_F} (\delta J_{AF})^2,\tag{22}$$

where h_c^+ and h_c^- are the middle critical field and are given

$$h_c^\pm = J_{AF} \left(1 + \frac{\alpha}{4} \pm \frac{2\delta^2}{\alpha} \right).\tag{23}$$

Summarizing, implementing two continuum filed theories we found that the model has four critical fields.

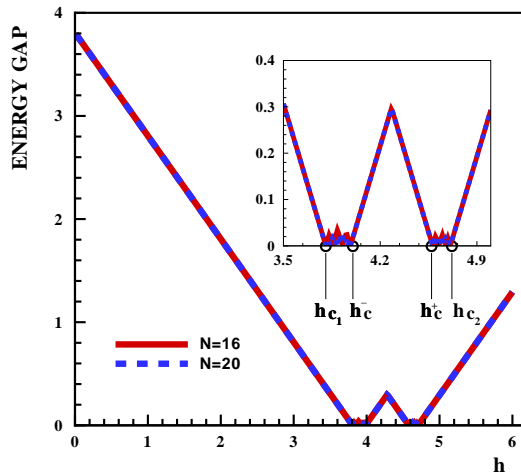


Figure 3. (Color online.) Difference between the two lowest energy levels of the original Hamiltonian versus the magnetic field h , for chains with different lengths $N = 16, 20$ and exchange parameters $J_F = 1.0$, $J_{AF} = 9/2$ and $\delta = 1/9$.

4. Numerical results

To explore the nature of the spectrum and the quantum phase transition, we have used Lanczos method to diagonalize numerically chains with length up to $N = 28$.

First, we have computed the three lowest energy eigenvalues of chains with $J_F = 1.0$, different values of the length and antiferromagnetic exchanges. To get the energies of the few lowest eigenstates we consider chains with periodic boundary conditions.

In Fig.3, we present results of these calculations for the exchanges $J_F = 1.0$, $J_{AF} = 9/2$, $\delta = 1/9$ and chain sizes $N = 16, 20$. We define the excitation gap as a gap on the first excited state. As it is seen in Fig. 3, in strong limit of antiferromagnetic exchange, this difference is characterized by the indistinguishable (within the used numerical accuracy) dependence on the chain length and shows an universal linear decrease with increasing magnetic field. At $h = 0$ the spectrum of the model is gapped. Turning the magnetic field the energy gap decreases linearly with h and vanishes at h_{c_1} . This is the first level crossing between the ground-state energy and the first excited state energy. The spectrum remains gapless for $h_{c_1} < h < h_c^-$, whereas the gap is reopened when $h > h_c^-$. After an increasing and a decreasing the spin gap goes to zero and vanishes at h_c^+ . More increasing in the field $h > h_c^+$, the spectrum remains gapless up to the critical saturation field h_{c_2} . Finally, at $h > h_{c_2}$ the gap is reopened and for a sufficiently large field becomes proportional to h . Oscillations of the energy gap in regions $h_{c_1} < h < h_c^-$ and $h_{c_2} < h < h_c^+$ are the result of level crossings in finite size systems. To find the critical fields we have used the phenomenological renormalization group (PRG) method [12]. The critical field values are given as follows:

$$h_{c_1} = 3.80 \pm 0.01, \quad h_{c_2} = 4.71 \pm 0.01,$$

$$h_{c^-} = 3.99 \pm 0.01, \quad h_{c^+} = 4.58 \pm 0.01. \quad (24)$$

To study the magnetic order of the ground state of the system, we start with the magnetization process. First, we have implemented the Lanczos algorithm on finite chains to calculate the lowest eigenstate. The magnetization along the field axis is defined as

$$M^z = \frac{1}{N} \sum_{j=1}^N \langle GS | S_j^z | GS \rangle, \quad (25)$$

where the notation $\langle GS | \dots | GS \rangle$ represents the ground state expectation value. In Fig. 4, we have plotted M^z as a function of the magnetic field h , and for a chain with exchange parameters $J_F = 1.0$, $J_{AF} = 9/2$, $\delta = 1/9$ and different lengths $N = 20, 24, 28$. As it is clearly seen in Fig. 4 besides the standard singlet and saturation plateaus at $h < h_{c_1}$ and $h > h_{c_2}$ respectively, we observe a plateau at $M = \frac{1}{2}M_{sat}$. Observed oscillations of the magnetization at $h_{c_1} < h < h_c^-$ and $h_c^+ < h < h_{c_2}$ result from the level crossing between the ground and the first excited states of this model in the gapless phases. To check that the mid-plateau is not a finite size effect, we performed the size scaling [37] of its width and found that the size of the plateau interpolates to finite value when $N \rightarrow \infty$. In the inset of Fig. 4 we have plotted the magnetization on site, $M_j^z = \langle GS | S_j^z | GS \rangle$, as a function of the site number "j" for a value of the magnetic field corresponding to the plateau at $M^z = 0.5M_{sat}^z$. To obtain an accurate estimate of the function M_j^z , we have calculated it for system sizes of $N = 12, 16, 20, 24, 28$. The thermodynamic limit ($N \rightarrow \infty$) of the finite size results are obtained by extrapolation method and used for plotting. As we observe the system shows a well pronounced modulation of the on site magnetization, where magnetization on odd bonds is larger than on even bonds. This distribution remains almost unchanged within the plateau for $h_c^- < h < h_{c^+}$.

By analyzing the numerical results on the energy gap (Fig. 3), we found that the spectrum is gapped in absence of the magnetic field which is one of the properties of the Haldane phase. The Haldane phase can be recognized from studying the string order parameter. The string correlation function in a chain of length N , defined only for odd l , is[38]

$$O_{Str}(l, N) = -\langle \exp\{i\pi \sum_{2j+1}^{2j+l+1} S_k^z\} \rangle. \quad (26)$$

In particular, we calculated the string correlation function for different finite chain lengths. Since the present model has a $SU(2)$ symmetry in the absence of a magnetic field, we only consider the z component of the string correlation function. In Fig. (5), we have plotted $O_{Str}(l, N)$ as a function of h for the chain with exchanges $J_F = 1.0$, $J_{AF} = 9/2$, $\delta = 1/9$ and lengths $N = 20, 24, 28$. As can be seen from this figure, at $h < h_{c_1}$, the string correlation function $O_{Str}(l, N)$ is saturated and the tetrameric chain system is in the Haldane phase. The Haldane phase remains stable even in the presence of a magnetic field less than h_{c_1} .

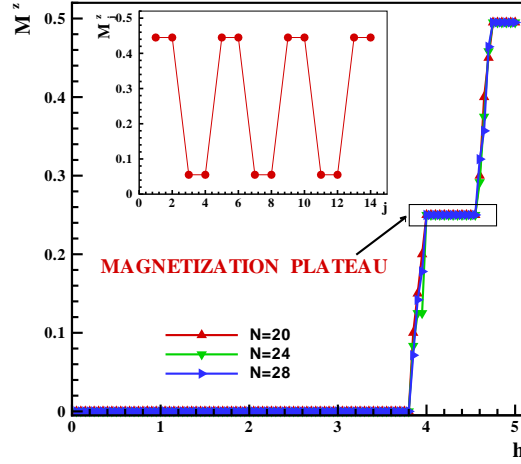


Figure 4. (Color online.) The magnetization along the field, M^z , as a function of the applied magnetic field h , for chains with exchanges $J_F = 1.0$, $J_{AF} = 9/2$, $\delta = 1/9$ and lengths $N = 20, 24, 28$. In the inset, the magnetization on site as a function of the site number j is plotted for a value of the magnetic field in the region of the to mid-plateau.

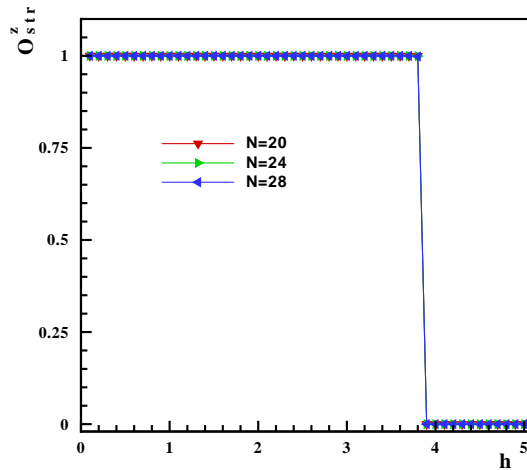


Figure 5. (Color online.) The string correlation function, $O_{Str}(l, N)$, as a function of the applied magnetic field h , for chains with exchanges $J_F = 1.0$, $J_{AF} = 9/2$, $\delta = 1/9$ and lengths $N = 20, 24, 28$.

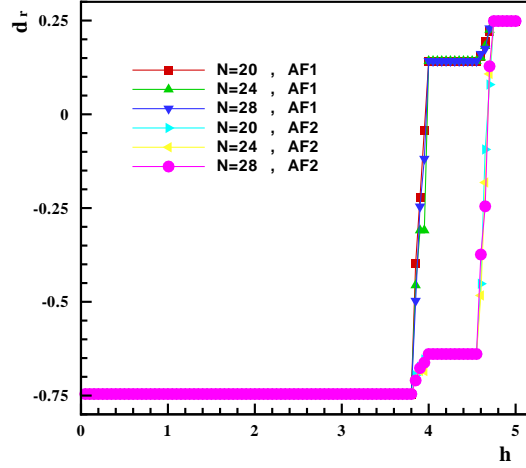


Figure 6. (Color online.) The AF-bond dimerization order parameter as a function of the applied field h , for chains with exchanges $J_F = 1.0$, $J_{AF} = 9/2$, $\delta = 1/9$ and lengths $N = 20, 24, 28$.

An additional insight into the nature of different phases can be obtained by studying the correlation functions. We define the following weak and strong bond dimerization order parameters;

$$d_r^w = \frac{4}{N} \sum_{j_{\text{odd}}=1,3,5,\dots}^{N/2} \langle GS | \mathbf{S}_{2j-1} \cdot \mathbf{S}_{2j} | GS \rangle, \quad (27)$$

and

$$d_r^s = \frac{4}{N} \sum_{j_{\text{even}}=2,4,6,\dots}^{N/2} \langle GS | \mathbf{S}_{2j-1} \cdot \mathbf{S}_{2j} | GS \rangle, \quad (28)$$

where summations are taken over the weak and strong antiferromagnetic-bonds. In Fig. (6) we have plotted d_r^w and d_r^s versus magnetic field h for chain of lengths $N = 20, 24, 28$ with the exchange parameters $J_F = 1.0$, $J_{AF} = 9/2$ and $\delta = 1/9$. As it is seen from this figure, at $h < h_{c_1}$ spins on all antiferromagnetic-bonds are in a singlet state $d_r^w = d_r^s \simeq -0.75$, while at $h > h_{c_2}$, d_r is equal to the saturation value $d_r^w = d_r^s \sim 1/4$ and the ferromagnetic long-range order along the field axis is present. However, in the considered case of strong antiferromagnetic exchanges ($J_{AF}^\pm \gg J_F$) and high critical fields quantum fluctuations are substantially suppressed and calculated averages of on-antiferromagnetic-bond spin correlations are very close to their nominal values.

On the other hand, for intermediate values of the magnetic field, at $h_{c_1} < h < h_{c_2}$ the data presented in Fig. (6) gives us a possibility to trace the mechanism of singlet-pair melting with increasing magnetic field. As it follows from Fig. (6) at h slightly above h_{c_1} spin singlets pairs start to melt in all antiferromagnetic bonds simultaneously and almost

with the same intensity. With further increase of h melting of weak antiferromagnetic-bonds gets more intensive, however at $h = h_c^-$ the process of melting stops. As it is seen in Fig. (6) weak antiferromagnetic-bonds are polarized, however their polarization is far from the saturation value $d_r^w \simeq 0.15$, while the strong antiferromagnetic-bonds still manifest strong on-site singlet features with $d_r^s \simeq -0.65$. Moratorium on melting stops at $h = h_c^+$, however for $h > h_c^+$ strong antiferromagnetic-bonds start to melt more intensively while the polarization of weak antiferromagnetic-bonds increases slowly. Finally at $h = h_{c_2}$ both subsystems of antiferromagnetic-bonds achieve an identical, almost fully polarized state. Note, that the almost symmetric fluctuations in on-antiferromagnetic-bonds correlations, increase in d_r^w at $h \leq h_c^-$ decrease in d_r^s at $h \geq h_c^+$ reflect the enhanced role of quantum fluctuations in vicinity of quantum critical points.

In our previous paper [13], we introduced a mean field order parameter which can distinguish a gapless LL phase from the other gapped phases. This order parameter is the F-dimer order parameter which is defined as

$$P_F = \text{Re}\langle S_{2n}^- S_{2n+1}^+ \rangle. \quad (29)$$

The F-dimer order parameter has a considerable value in the Luttinger liquid phase and behaves differently in the other gapped phases. The effects of a small value of space modulation on this parameter has been shown in Fig. (7). We have plotted P_F versus magnetic field h for chain of lengths $N = 12, 16, 20,$ and 24 with the exchange parameters $J_F = 1.0$, $J_{AF} = 9/2$, and $\delta = 1/9$. As it is seen, in the Haldane phase, $h < h_{c_1}$, the quantum fluctuations suppress the ferromagnetic correlations and the F-dimer parameter is close to zero-value. Right after the first critical field, the F-dimer parameter increases rapidly up to the second critical field. In the intermediate region, $h_{c^-} < h < h_{c^+}$, the F-dimer parameter shows a non-zero plateau which behavior is the same as the other parameters. By more increasing field, the F-dimer decreases and goes to zero at the saturation critical field $h = h_{c_2}$. The intermediate region is a gapped phase and we expect the zero-value for the defined LL parameter, P_F . However the gap does not affect on the behavior of P_F and a plateau appears in the curve.

5. Pair-wise entanglement

In this section we focus on the entanglement of two spins in different phases of the system. The entanglement which has no a classical counterpart is employed to study the quantum correlations of different states. Concurrence is a measure of the bipartite entanglement which is defined as following [39, 40]

$$C_{lm} = 2 \max\{0, C_{lm}^{(1)}, C_{lm}^{(2)}\}, \quad (30)$$

where

$$C_{lm}^{(1)} = \sqrt{(g_{lm}^{xx} - g_{lm}^{yy})^2 + (g_{lm}^{xy} + g_{lm}^{yx})^2} \\ - \sqrt{\left(\frac{1}{4} - g_{lm}^{zz}\right)^2 - \left(\frac{M_l^z - M_m^z}{2}\right)^2},$$

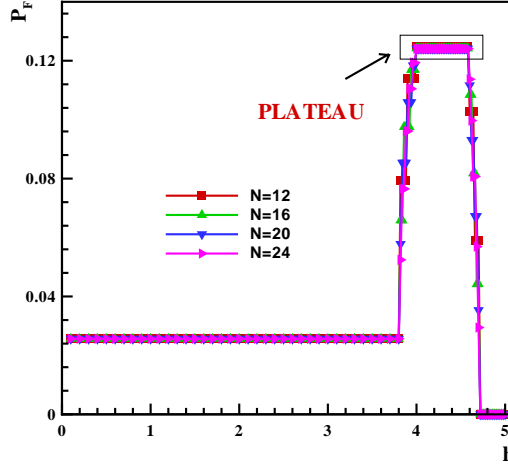


Figure 7. (Color online.) The F-dimer order parameter as a function of the applied field h , for the chains with exchanges $J_F = 1.0$, $J_{AF} = 9/2$, and $\delta = 1/9$ and lengths $N = 12, 16, 20$, and 24 . The appearance of a non-zero plateau in the curve is clear.

$$C_{lm}^{(2)} = \sqrt{(g_{lm}^{xx} + g_{lm}^{yy})^2 + (g_{lm}^{xy} - g_{lm}^{yx})^2} - \sqrt{\left(\frac{1}{4} + g_{lm}^{zz}\right)^2 - \left(\frac{M_l^z + M_m^z}{2}\right)^2} \quad (31)$$

and $g_{lm}^{\alpha\beta} = \langle S_l^\alpha S_m^\beta \rangle$ is the correlation function between spins l and m . The numerical Lanczos results on the concurrence for the 1D tetrameric spin-1/2 model have been shown in Fig. (8). We have plotted the entanglement of two spins which are located at the same strong, weak, and ferromagnetic bond versus h , chain length $N = 28$ and the exchange parameters $J_F = 1.0$, $J_{AF} = 9/2$, and $\delta = 1/9$. In the Haldane phase, $h < h_{c_1}$, the spins on all antiferromagnetic bonds make a singlet state. In this state which is a maximally entangled state, $g_{lm}^{xx} = g_{lm}^{yy} = g_{lm}^{zz} = \frac{-1}{4}$, $C^S = C^W = 1$, and C^F is zero. For $h > h_{c_1}$ the values of C^S and C^W fall down with increasing of the magnetic field. Indeed the quantum correlations of the two spins with strong antiferromagnetic (SSA) and weak antiferromagnetic (SWA) interactions are decreased by increasing the magnetic field. However an enhancement on the entanglement of the two spins with ferromagnetic interaction (SF) is observed. It means that the magnetic field increases the quantum correlations of the two spins which are interacting ferromagnetically. This is a dual effect of the magnetic field in which increases the quantum correlations of two SF and decreases the quantum correlations of two SWA and two SSA. In the intermediate gapless region $h_{c_1} < h < h_{c_-}$, the quantum correlations of SWA and SSA diminish down to $h = h_{c_-}$ and the concurrences C^W and C^S reduce to ~ 0.1 and ~ 0.9 respectively. However, the quantum correlations of SF grows up to the critical field h_{c_-} and the entanglement reach to the value ~ 0.25 . At the plateau state, the gap of the system is re-opened and a plateau emerges in the curve of concurrences. In the intermediate gapped phase the values of the concurrences C^S , C^W , and C^F are 0.9, 0.1, and 0.25,

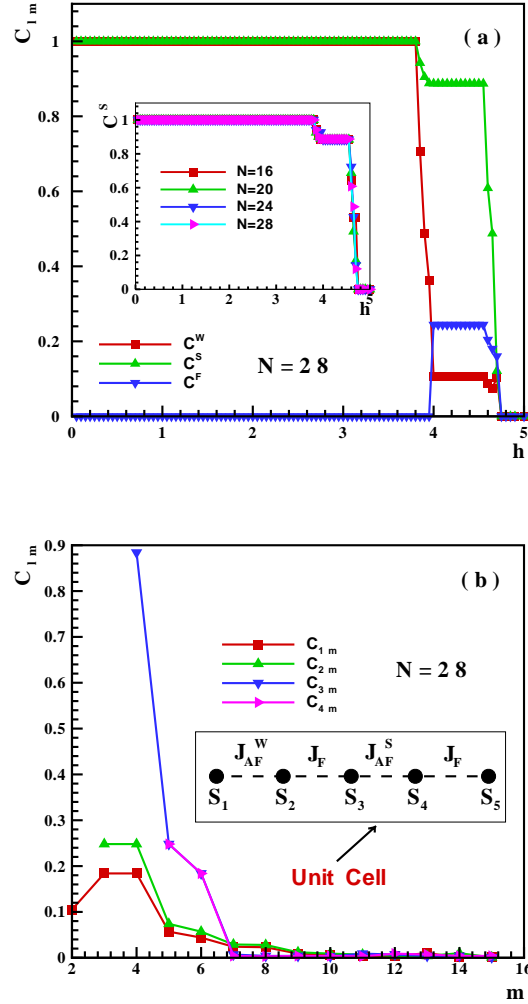


Figure 8. (Color online.) (a)-The concurrence as a function of the applied field h , for chains with exchanges $J_F = 1.0$, $J_{AF} = 9/2$, and $\delta = 1/9$ and length $N = 28$. Inset plot: The concurrence between two spins on strong bond as a function of h for different chain sizes $N = 16, 20, 24$, and 28 . (b)- Concurrence of two spins versus separation distance m .

respectively. Indeed in the plateau state there are three types of quantum correlations in the system. These correlators are the source of the mid-plateaus in the different parameters of the system such as magnetization, bond dimer and F-dimer parameters. Indeed all of these quantum correlators exist only at the mid-plateau states. In the full saturated state all of them disappear and the entanglement of the state is exactly zero.

To see the finite size effects, we have plotted in the inset plot of Fig. 8(a), the concurrence between two SSA as a function of h for different chain sizes $N = 16, 20, 24$, and 28 . It can be seen that there is not size effect on the numerical results and the concurrence behaves as thermodynamic limit in the gapped regions.

To get more intuition on the mid-plateau state, we have computed numerically the entanglement between the spins with different separation distances. The concurrence between a SSA and an arbitrary spin, say S_m has been plotted versus the separation distance m , in Fig. 8(b). The entanglement of two such spins is decreased by increasing m and goes to zero at the finite value of $m = 7$. The same behavior is also observed for the entanglement between a SWA and the spin S_m with respect to m . The entanglement between SWA and S_m goes to zero at $m = 9$. It means that, in the plateau state the range of the quantum correlations between a SWA and S_m is longer than the range of a SSA and S_m . This is the other feature of the mid-plateau state.

It is also remarkable that from our numerical results we found that the concurrence of two spins that are not on the same bond is equal to zero in the gapped Haldane and saturated ferromagnetic phases which is in complete agreement with the analytical results.

6. conclusion

In this paper, we have focused on the magnetic properties of a bond-alternating antiferromagnetic-ferromagnetic spin-1/2 Heisenberg chain. Using two analytical approaches and a numerical method we have studied the effects of an external magnetic field and a space modulation on the ground state properties of the system. In the limit where the AF couplings are dominant, we mapped the model (1) to an effective XXZ Heisenberg chain with anisotropy parameter $\Delta = 1/2$ in the presence of effective uniform and staggered longitudinal magnetic fields. This model has different quantum phases which are distinguished by four critical fields. To find the critical fields we employed two field theoretical approaches such as nonlinear sigma model and bosonization, and the numerical exact daigonalization Lanczos method. Working on the spin coherent states representation, we mapped the model (1) to a nonlinear sigma model with an additional topological term. The topological term is dependent on the space modulation δ and the parameter $\alpha = \frac{J_F}{J_{AF}}$. For any values of α and δ , the Hamiltonian mapped to a non-integrable $O(3)$ NL σ M with Θ in the interval $[0, \pi]$. In the absence of a magnetic field the model is always gapped and the gap value depends to α and δ . By analyzing our NL σ M in presence of the magnetic field, we obtained only the two critical fields. To dominant this vacancy and to find the other two critical fields we also bosonized the effective Hamiltonian of XXZ chain (3). Our bosonization procedure showed that the width of the mid-plateau is a function of δJ_{AF} . It has been shown that the plateau-width, scales as a power low with exponent value 2 and vanishes at $\delta = 0$.

Moreover, we implemented the Lanczos method to numerically diagonalize chains with finite length up to $N = 28$. Using the exact diagonalization technique, we calculated the energy gap, magnetization, the string, the F-dimer, and the bond dimer order parameters and various correlation functions for different values of the external magnetic field. In good qualitative agreement with our analytical results, we showed clearly that a space modulation on the antiferromagnetic exchanges leads to generation

of a gap in the excitation spectrum of the system and correspondingly a magnetization mid-plateau at $\frac{M}{M_{sat.}} = \frac{1}{2}$. We found that a non-zero plateau also creates in the plot of F-dimer, bond dimer order parameters.

To get more physical insight on the mid-plateau state we also investigated the pair-wise entanglement between two different spins of the system. As a measure of entanglement the concurrence between two arbitrary spins computed as a function of magnetic field. A plateau is also appeared in the concurrence at the middle gapped state. In the plateau state there are three types of quantum correlations in the system. in the plateau state the range of the quantum correlations between a spin on the weak antiferromagnetic bond and a S_m is longer than the range of the quantum correlations of a spin on the strong antiferromagnetic bond and S_m .

7. Acknowledgments

JA thanks A. Langari for his fruitful suggestions on the manuscript. We are grateful to G. I. Japaridze and T. Vekua for their useful comments.

References

- [1] Haldane F D M, 1983 *Phys. Rev. Lett.* **50**, 1153.
- [2] Oshikawa M, Yamanaka M and Affleck I, 1997 *Phys. Rev. Lett.* **78**, 1984.
- [3] Takada S, 1992 *J. Phys. Soc. Jpn.* **61**, 428.
- [4] Hida K and Takada S, 1992 *J. Phys. Soc. Jpn.* **61**, 1879.
- [5] Hida K, 1993 *J. Phys. Soc. Jpn.* **62**, 439.
- [6] Hida K, 1992 *Phys. Rev. B* **46**, 8268.
- [7] Kohmoto M and Tasaki H, 1992 *Phys. Rev. B* **46**, 3486.
- [8] Yamanaka M, Hatsugai Y, and Kohmoto M, 1993 *Phys. Rev. B* **48**, 9555.
- [9] K. Hida, 1994 *J. Phys. Soc. Jpn.* **63**, 2514.
- [10] T. Sakai, 1995 *J. Phys. Soc. Jpn.* **64**, 251.
- [11] Yamamoto S and Funase K, 2005 *Low Temp. Phys.* **31**, 740.
- [12] Mahdavifar S and Akbari A, 2008 *J. Phys. Soc. Jpn.* **77**, 024710.
- [13] Abouie J and Mahdavifar S, 2008 *Phys. Rev. B* **78**, 184437.
- [14] Ajiro Y, Asano T, Inami T, Aruga-Katori H and Goto T, 1994 *J. Phys. Soc. Jpn.* **63**, 859.
- [15] K. Hida, 1994 *J. Phys. Soc. Jpn.* **63**, 2359.
- [16] K. Okamoto, 1996 *Solid State Commun.* **98**, 245.
- [17] Bo Gu, Gang Su and Song Gao, 2006 *Phys. Rev. B* **73**, 134427.
- [18] Shou-Shu Gong, Bo Gu and Gang Su, 2008 *Phys. Lett. A* **372**, 2322.
- [19] Escuer A, Vicente R, El Fallah M S, Goher M A S and Mautner F A, 1998 *Inorg. Chem.* **37**, 4466.
- [20] Lu H T, Su Y H, Sun L Q, Chang J, Liu C S, Luo H G, and Iang T, 2005 *Phys. Rev. B* **71**, 144426.
- [21] Gong Shou-Shu, Gao Song and Su Gang, 2009 *Phys. Rev. B* **80**, 014413.
- [22] Stone M B, Tian W, Lumsden M D, Granroth G E, Mandrus D, Chung J -H, Harrison N, and Nagler S E, 2007 *Phys. Rev. Lett.* **99**, 087204.
- [23] Chen Wei, Hida Kazuo and Nakano Hiroki, 1998 *J. Phys. Soc. Jpn.* **68**, 625.
- [24] Mila F, 1998 *Eur. Phys. J. B* **6**, 201.
- [25] Alcaraz F C and Malvezzi A L, 1995 *J. Phys. A: Math Gen* **28**, 1521.
- [26] Okamoto K and Nomura K, 1996 *J. Phys. A: Math Gen* **29**, 2272.
- [27] Japaridze G I and Pogossyan E, 2006 *J. Phys.: Condens. Matter* **18**, 9297; Japaridze G I, Mahdavifar S, 2009 *Eur. Phys. J. B* **68**, 59.

- [28] Fouet J -B, Tchernyshyov O, Mila F, 2004 *Phys. Rev. B* **70**, 174427.
- [29] Mahdaviifar S, 2007 *Eur. Phys. J. B* **55**, 371.
- [30] Bosquet M and Jolicoeur th, 2000 *Eur. Phys. J. B* **14**, 47.
- [31] Loss D and Maslov D L, 1995 *Phys. Rev. Lett.* **74**, 178.
- [32] Normand B, Kyriakidis Jordan and Loss Daniel, 2000 *Ann. Phys. (Leipzig)* **9**, 133.
- [33] Eggert S and Affleck I, 1992 *Phys. Rev. B* **46**, 10866.
- [34] Hikihara T and Furusaki A, 1998 *Phys. Rev. B* **58R**, 583.
- [35] Zamolodchikov Al B, 1995 *Int. J. Mod. Phys. A* **10**, 1125.
- [36] Japaridze G I and Nersesyan A A, 1978 *JETF Pis'ma* **27**, 356; Japaridze G I and Nersesyan A A, 1978 *JETP Lett.* **27**, 334; Japaridze G I and Nersesyan A A, 1979 *J. Low Temp. Phys.* **37**, 95; Pokrovsky V L and Talapov A L, 1979 *Phys. Rev. Lett.* **42**, 65.
- [37] Zhitomirsky M E, Honecker A, Petrenko O A, 2000 *Phys. Rev. Lett.* **85**, 027207.
- [38] Hida K, 1999 *Phys. Rev. Lett.* **83**, 3297.
- [39] Wooters W K, 1998 *Phys. Rev. Lett.* **80**, 2245.
- [40] Amico L, Fazio R, Osterloh A, and Vedral V, 2008 *Rev. Mod. Phys.* **80**, 517.